# CHEMICAL ENGINEERING JOURNAL

(This is a sample cover image for this issue. The actual cover is not yet available at this time.)

# Mechanism of Pb$^{2+}$ removal from aqueous solution using a nonliving moss biomass

Bamidele I. Olu-Owolabi [a], Paul N. Diagboya [a,*], William C. Ebaddan [b]

[a] Department of Chemistry, Faculty of Science, University of Ibadan, Ibadan, Nigeria
[b] Department of Agronomy, Faculty of Agriculture, University of Ibadan, Ibadan, Nigeria

## HIGHLIGHTS

▶ The moss plant *Barbula lambarenensis* (RBL) will be useful for metal adsorption from aqueous solution.
▶ The maximum adsorption capacity ($Q_o$) for Pb adsorption is 62.50 mg/g at 298 K and 90.91 mg/g at 323 K.
▶ The pH for optimum adsorption is 5.0 while maximum adsorption was attained in 30 min.
▶ The adsorption data obeyed the pseudo-second-order model.
▶ The free energy changes ($\Delta G^o$) are positive and the reaction is exothermic.

## ARTICLE INFO

## ABSTRACT

Biosorption of lead (II) ions onto raw biomass of the moss plant *Barbula lambarenensis* has been studied using the batch equilibrium adsorption method. Equilibrium isotherms, kinetics and thermodynamic parameters have been evaluated. The FT-IR analysis showed that likely functional groups responsible for the adsorption are carboxyl, carbonyl, amides and hydroxyl groups. The pH for optimum adsorption is 5.0. Equilibrium data fit well to the Langmuir isotherm. The estimated maximum adsorption capacity was found to be 62.50 mg/g at 298 K and 90.91 mg/g at 323 K. The kinetic data obeyed the pseudo-second-order model. The free energy changes ($\Delta G^o$) are positive and the reaction is exothermic with decreased randomness at the sorbent/solution interface. Taking into account its good adsorption capacity, ease of sample treatment, as well as availability, the biomass of *B. lambarenensis* is a promising cost-effective biosorbent for Pb$^{2+}$ removal from aqueous environment.

## 1. Introduction

Several techniques have been employed for metal ions removal from water: filtration, chemical precipitation, ion exchange, reverse osmosis, electrochemical treatment, membrane technology, evaporation recovery, solvent extraction, adsorption on activated carbon, etc. [1]. But these techniques are limited by techno-economic considerations as well as environmental friendliness. The ability of biomaterials to remove heavy metals through biosorption has proved to be highly efficient, easy to handle, environment-friendly, and economically feasible. This has attracted plenty of attentions in recent years [2–4] because biomaterials are: (i) available in abundance and cheap, (ii) easy to obtain and process, and (iii) available as waste type or nuisance [5].

Several workers have investigated and reported various plant materials' ability to adsorb different metals from solution. These include mungbean husk [5], hazelnut shell [6], almond shell [6], pine [7], lignin [8], tea leaves [9], tree fern [10], groundnut husks [11], sphagnum moss peat [12], sawdust [13], rice hulls [14], chitosan [14], sugarcane bagasse [15], cocoa shell [16], and rice husk [17]. However, some major limitations of these biosorptions are that some of them have not yielded satisfactory results (high metal adsorption capacity) and others that yielded good results may not locally be available.

Biosorption involves one or more of several processes including metal ion coordination complex, ion exchange, and covalent linkage to biomass components. However, biomass of different origins have different sorption capacities because of their different affinities for different metals; and since there is no way to predict metal sorption capacity of a certain biomass, the search for an ideal techno-economically feasible biosorbent, that meets the above listed criteria is continuing [5].

There has been no reported work on Pb$^{2+}$ removal from aqueous solution using the moss *Barbula Lambarenensis* (BL). Ogunfowokan

---

* Corresponding author. Present address: National Center for Nanoscience and Nanotechnology, Beijing 100190, China. Tel.: +86 18310212731, +234 8038052553.
*E-mail address:* pauldn2@yahoo.com (P.N. Diagboya).

et al. [18] have shown the living biomass of BL is a bio-indicator of heavy metals in the environment. This may be an indication of the ability of the dead biomass to adsorb these metals. Since BL is abundantly available at no cost, and $Pb^{2+}$ pollution of surface waters is a major international challenge, the BL was investigated for the development of a BL-based procedure for the removal of $Pb^{2+}$ from aqueous solution.

In this study, the sorption behavior of $Pb^{2+}$ from aqueous solution using BL was studied under various conditions; contact time, solution pH, temperature and sorbent dose, and sorbate concentration, with the aim of determining the mechanism for the removal of $Pb^{2+}$ from aqueous solution by biomass of *B. Lambarenensis*.

## 2. Methodology

### 2.1. Sampling, pre-treatment and characterization of biosorbent material

The *B. Lambarenensis* was obtained in August 2011 in Agbor (6°11'6''E; 6°15'9''N), Delta State, Nigeria; washed severally with tap water and deionized water to remove impurities, then air-dried, ground, sieved through a 0.5 mm mesh size sieve, and the sieved particles were used for the study. This was called the raw BL (RBL).

The Specific Surface Area (SSA) of the sample was determined using the methods of Sears [19] and Iler [20]. The bulk density and specific gravity of the RBL sample was determined as described by Radojevic and Bashkin [21]. The pH at the point zero charge (pH PZC) was determined as described by Unuabonah et al. [22]. The determination of RBL surface properties is necessary because the particle sizes are most likely heterogeneous and these properties aid in estimating the degree of metal sorption. The SSA of RBL has been determined as 11.352 $m^2$/g, while the bulk density and specific gravity are 0.424 g/$cm^3$ and 0.172 g/$cm^3$, respectively. The pH PZC value is 7.01. This is important because it marks the pH where the surface functional groups do not contribute to the pH of the solution, and in an applied electric field, the electrophoretic mobility of the particles would be zero [23].

The Fourier Transform Infrared (FTIR) spectra of the RBL biosorbent were obtained using Perkin Elmer Spectrum 1 FTIR spectrophotometer. About 0.1 g of the processed dry RBL biosorbent in powder form along with KBr were ground into fine particles and pressed to make pellets with was used to obtain the FT-IR spectrum in the scanning frequency from 4500 to 500 $cm^{-1}$.

### 2.2. Biosorption procedures

1000 mg/L of standardized $Pb^{2+}$ stock solution was prepared from the analytical grade chloride salt. Working solutions of required concentrations were prepared from this stock as required. Replicate batch experiments were used to determine metal sorption capacity of the biomass in 60 mL polyethylene bottles by contacting approximately 0.1 g of the RBL biomass with 20 mL of metal solution, except where otherwise stated, for determining effect of pH, time, temperature and sorbate concentration. The sorbent–sorbate mixtures were shaken on a mechanical shaker during the course of the adsorption experiment and concentrations of metal in the filtrate solutions were determined using the Buck Scientific 205 Atomic Absorption Spectrometer (AAS) with air-acetylene flame on absorbance mode.

The quantity of metal adsorbed by RBL after each specified incubation period was calculated using the following equation:

$$Q = \frac{(C_o - C_e)V}{M} \qquad (2.1)$$

where $Q$, $C_o$ and $C_e$ are the cation adsorbed (mg/g), the initial and equilibrium metal concentrations in the solution (mg/L),

respectively; and $V$ (mL) and $M$ (g) are respectively the volume of solution and mass of adsorbent.

To obtain insights into the surface properties and degree of affinity of RBL, sorption data were tested against the Langmuir, Freundlich and Dubinin–Radushkevich equilibrium isotherms using the linear forms of these models in Eqs. (2.2) and (2.3).

$$\text{Langmuir}: \quad \frac{C_e}{q_e} = \frac{1}{Q_o b} + \frac{C_e}{Q_o} \quad \text{(Linear form)} \qquad (2.2)$$

$$\text{Freundlich}: \log q_e = \log K_f + \frac{1}{n}\log C_e \quad \text{(Linear form)} \qquad (2.3)$$

where $Q_o$ (mg/g) and $q_e$ is the maximum adsorption and amount of solute adsorbed per unit weight of adsorbent (mg/g), respectively. $C_e$, is same as above; $b$, $K$, and $n$ are isotherm constants obtained from the slopes and intercepts.

The Dubinin–Radushkevich isotherm which describes adsorption on both homogenous and heterogeneous surfaces [24] is shown in the following equation:

$$In q_e = In X_m - \beta \varepsilon^2 \qquad (2.4)$$

where $X_m$ and $\beta$ are the Dubinin–Radushkevich monolayer adsorption capacity (mg/g) and the constant related to sorption energy respectively, and $\varepsilon$ is the Polanyi potential which is related to the equilibrium concentration (Eq. (2.5)).

$$\varepsilon = RT In \frac{1}{C_e} \qquad (2.5)$$

In describing the kinetics of the biosorption, the pseudo-first-order, pseudo-second-order, Elovich, and Intra-particle diffusion models have been applied to the biosorption data. The Lagergren pseudo-first-order and pseudo second-order rate equations [25] were tested using their simplified equations in (2.6) and (2.7) respectively:

$$\log(q_e - q_t) = \log q_e - \frac{k_1}{2.303}t \qquad (2.6)$$

where $q_e$ and $q_t$ are the amounts of metals sorbed (mg/g) at equilibrium and at time $t$, respectively; and $k_1$ is the rate constant of pseudo-first-order sorption ($min^{-1}$). The $q_e$ and rate constants $k_1$ were calculated from the slope and intercept of the plot of log $(q_e - q_t)$ vs. $t$.

$$\frac{t}{q_t} = \frac{1}{k_2 q_e^2} + \frac{t}{q_e} \qquad (2.7)$$

where $k_2$ is the rate constant of pseudo-second-order sorption. The pseudo-second-order rate constants $k_2$ and $q_e$ values were calculated from the slope and intercept of the plots $t/q$ vs. $t$.

The Elovich model equation [26] in Eq. (2.8) was used.

$$q_t = \frac{1}{\beta} In(\alpha\beta) + \frac{1}{\beta} In(t) \qquad (2.8)$$

where $\alpha$ is the initial adsorption rate (mg/g/min) and $\beta$ is the desorption constant (g/mg) during any one experiment.

The linearized form of the intra-particle diffusion model equation [26] was used as shown in Eq. (2.9).

$$\log R = K_{id} + \alpha \log(t) \qquad (2.9)$$

where $R$ is percentage metal ion adsorbed, $t$ is contact time, $\alpha$ is gradient of linear plots and depicts the adsorption mechanism, $K_{id}$ is intra-particle diffusion rate constant ($h^{-1}$)

The biosorption thermodynamic parameters; enthalpy ($\Delta H^o$), entropy ($\Delta S^o$), Gibbs free energy ($\Delta G^o$) and equilibrium constant ($Kc$), were determined for the experimental systems using Eqs. (2.10)–(2.12), plotting graph of $In K_c$ verses $1/T$ and using the slope and intercept to evaluate the values of $\Delta H^o$ and $\Delta S^o$.

$$K_c = \frac{q_e}{C_e} \tag{2.10}$$

$$\Delta G^o = -RT \ln K_c \tag{2.11}$$

$$\ln Kc = -\frac{\Delta H^o}{RT} + \frac{\Delta S^o}{R} \tag{2.12}$$

## 3. Results and discussion

### 3.1. Fourier Transform Infrared (FT-IR) spectroscopy

FT-IR test spectra of unloaded RBL biomass showed several absorption peaks between the scanning frequency range of 4500–500 cm$^{-1}$ (Fig. 1). The broad band positioned around 3400 cm$^{-1}$ is indicative of the stretching band of the carbonyl double bond from some carboxylic acids and their salts, a stretching vibration of free hydroxyl functional groups of aromatic and aliphatic origins, and possibly N—H stretch of amides. The water content in the RBL biomass and the numerous free hydroxyl groups in the polysaccharide structure of this moss plant wall may explain the presence of the band. The sharp absorption just below 3000 cm$^{-1}$ is indicative of C—H stretch likely from alkanes while the band at around 2350 cm$^{-1}$ is suggestive of cumulative double bonds stretch of O=C=O. The band around 1700 is characteristic of the C=O stretch of carbonyl double bond either from free or esterified carboxyl groups. However, closer band frequencies at 1655 cm$^{-1}$ have been attributed to amide-I of protein secondary structures. The absorption peak at about 1424 cm$^{-1}$ suggests aromatic methyl group/methyl ketone and carboxylate vibrations or likely C—H deformations of alkanes. The strong band around 1090 cm$^{-1}$ is due likely to the C—OH bond and —C—C— stretchings, which are characteristic for polysaccharides. Peaks below 1000 cm$^{-1}$ have been attributed to such groups as aromatic C—H bending vibrations (874 cm$^{-1}$), thioesters (672 cm$^{-1}$), but majorly plane deformations. Similar observations have been reported by Yan et al. [4], Pehlivan et al. [6], Chakravarty et al. [27] and Yao et al. [28].

The pristine RBL spectra and that of the Pb$^{2+}$-loaded were compared. Although the spectra were similar, the peaks frequency and intensity of most functional groups in the Pb-loaded RBL were shifted slightly than those in the pristine; for instance, some characteristic peak locations of RBL shifted from 3421, 1638, 1513, 1426, 1078, 1035, 795, and 692 cm$^{-1}$ to 3413, 1639, 1516, 1428, 1076, 1036, 769, and 694 cm$^{-1}$, respectively, after Pb$^{2+}$ ions adsorption (peak values not shown in Fig. 1). These shifts may be attributed to the counter ions changes associated with the respective functional groups anions when they act as proton donors, suggesting their participation in Pb$^{2+}$ ion adsorption [4,6,27]. No marked change in frequency was observed between both spectra in the region just below 3000 cm$^{-1}$ (hydroxyl functional groups). However, the broadening of the peak in the pristine decreases indicating that the hydrogen bonding of the hydroxyl groups decreases after Pb adsorption. These observations suggest the involvement of carboxyl, carbonyl, thioesters, amides and hydroxyl functional groups in Pb$^{2+}$ ions biosorption.

### 3.2. Effect of pH on adsorption

Establishing the capacity of RBL as new biosorbent material for Pb$^{2+}$ requires knowing the optimum pH for adsorption. This was determined by equilibrating the sorbent–sorbate mixture containing 500 mg/L of Pb$^{2+}$ at pH values between 3 and 7. pH is an important biosorption parameter because it affects the activities of functional groups present on the surface of the biosorbent which are responsible for adsorption, and affects competitive adsorption of ions to sorption sites [7,24,26]. Thus, various biosorbents have various optimum sorption pH for different metals.

As shown in Fig. 2, the uptake of Pb$^{2+}$ ions is pH dependent. At the low pH value of 3.0, RBL adsorbed lower amount (56.4 mg/g or 57.8%) of Pb$^{2+}$ onto its surface active adsorption sites. With increase in solution pH, the quantity adsorbed increased steadily until pH 5.0 (70.6 mg/g or 71.6%) and 6.0 (72.4 mg/g or 73.3%) where the quantities of Pb$^{2+}$ adsorbed made a plateau on the graph before precipitation of Pb$^{2+}$ ions set in. In summary, steady increment in adsorption was observed from pH 3.0 to 5.0, indicating that more Pb$^{2+}$ ions were adsorbed on RBL surfaces as pH increased. Then adsorption reached a plateau between pH 5.0 and 6.0. The optimum pH for adsorption of Pb$^{2+}$ was recorded at pH 5.0. Above this pH, there was an apparent increase in adsorption of Pb$^{2+}$. This has been attributed mainly to solvation and hydrolysis of Pb$^{2+}$ ion products leading to precipitation of Pb$^{2+}$ from solution. In aqueous solutions of pH less than 5, Pb$^{2+}$ ions exist as either Pb$^{2+}$ or Pb(OH)$^+$ or both. However, the formation of Pb$^{2+}$ hydrolysis products begins to occur at pH values between 5 and 6, and this brings about precipitation. Due to this reason all the experiments were carried out at pH 5.

### 3.3. Adsorption kinetics

The efficiency of RBL to remove Pb$^{2+}$ metal from solution can be assessed by the rate of Pb$^{2+}$ adsorption, and may be linked to its
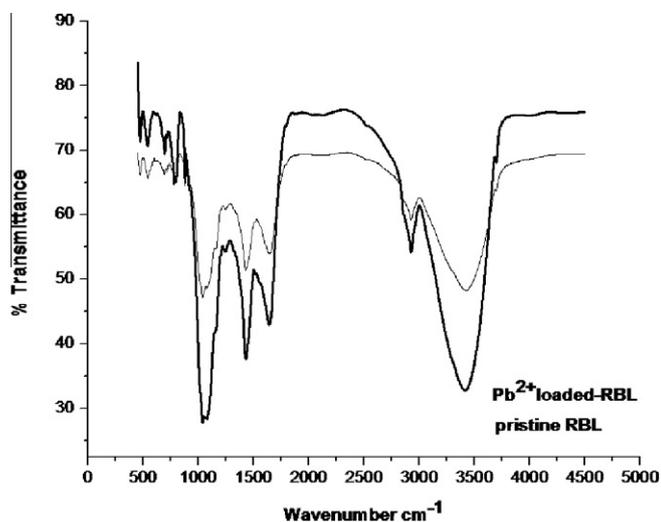


Fig. 1. FTIR spectra of raw *Barbula Lambarenensis* (RBL).
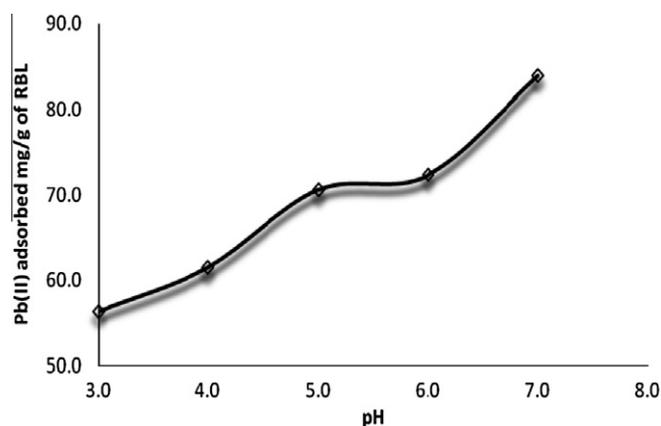


Fig. 2. Effect of pH on Pb$^{2+}$ adsorption.

efficiency to cleanup waste water. The effect of time (5, 15, 30, 60, 180, 360, and 720 min) on $Pb^{2+}$ sorption was determined by equilibrating the RBL-sorbate aliquot at pH 5.0 using 500 mg/L $Pb^{2+}$ solution. From the adsorption rate curve (Fig. 3), it was observed that $Pb^{2+}$ adsorption was rapid and nearly completed in 30 min with 71.7% (70.8 mg/g) of the total $Pb^{2+}$ in solution adsorbed. As time elapsed, there was little or no adsorption until after 720 min when the percentage of $Pb^{2+}$ adsorbed increased to 76.2% (75.3 mg/g). This trend of adsorption may be explained thus: the initial rapid increase in $Pb^{2+}$ uptake is due to the fact that a large number of vacant RBL surface sites are available for adsorption during the initial stage and since these have very high affinity for $Pb^{2+}$, they are filled rapidly; after this initial rapid adsorption, the remaining vacant surface sites become very difficult to occupy due to the repulsive forces between the solute molecules on the solid and bulk phases. This result has shown that the breaking of these repulsive forces barrier and further adsorption are time dependent as seen after 720 min. Hence, the time required to attain a rapid equilibrium is 30 min. However, a contact time of 720 min has been employed for every other study because of this possibility of further adsorption.

Four kinetics models have been used to test the mechanism that controlled the sorption process: the pseudo-first order, pseudo-second order, Elovich and intra-particle diffusion models. Table 1 showing the comparative fits of the various models indicates that the kinetics data fit the pseudo-second-order kinetics better than for pseudo-first-order kinetics because the $r^2$ value as well as the experimental $q_e$ value of the pseudo-second-order is better correlated implying that $Pb^{2+}$ adsorption is controlled by chemisorption involving sharing or exchange of electrons between sorbent and sorbate [29]. Intra-particle diffusion and Elovich models gave further insight into the kinetics models. Elovich curve, which did not pass through the origin (figure not shown), indicates there is some degree of boundary layer control. The linear intra-particle model also suggests that intra-particle diffusion is not the rate-controlling step [30].

### 3.4. Effect of adsorbent dose

The effect of adsorbent dose on adsorption was evaluated by equilibrating the sorbent–sorbate mixture with 500 mg/L of $Pb^{2+}$ at pH 5.0 using varying masses in the range of 0.05–0.5 g. It was observed (Fig. 4) that increasing the biomass dosage from a range 0.05 g through 0.50 g increased the percentage of $Pb^{2+}$ removal from aqueous solution from 49.69% to over 99%, while on the other hand, the equilibrium adsorption capacity, $q_e$, per mass of RBL was

**Table 1**
Sorption kinetics parameters.

| Model | Calculated parameters | Experimental value | $r^2$ |
|---|---|---|---|
| Pseudo-first-order | $q_e$ = 21.68 mg/g $K_1$ = 0.009 g/mg/min | $q_e$ = 75.28 mg/g | 0.828 |
| Pseudo-second-order | $q_e$ = 76.92 mg/g $K_2$ = 0.002 g/mg/min | $q_e$ = 75.28 mg/g | 0.998 |
| Elovich | $q_e$ = 57.34 mg/g $\beta$ = 0.19 | $q_t$ = 75.28 mg/g | 0.715 |
| Intra-particle diffusion | $R$ = 80.36% $\alpha$ = 0.091 $K_{id}$ = 1.645 | $R$ = 76.15% | 0.702 |

found to decrease (98.26–19.94 mg/g) with increase biomass dose. Similar reports are found in literature [7,22]. It is apparent that by increasing the amount of RBL, available sorption sites for sorbent–solute interaction is increased due to increased available surface negative charges and decrease in the electrostatic potential near the RBL surface which favors sorbent–solute interaction; hence, leading to the noticed increased percentage $Pb^{2+}$ removal from the aliquot solution. Unuabonah et al. [22] have attributed the $q_e$ decrease with increasing mass to the decreasing total surface area of the adsorbent and an increase in diffusion path length due to aggregation of RBL particles, and as the weight of the RBL increased, the aggregation becomes increasingly significant.

**Fig. 4.** Effect of varying biosorbent dose on $Pb^{2+}$ adsorption.

**Fig. 3.** Effect of time on $Pb^{2+}$ adsorption.
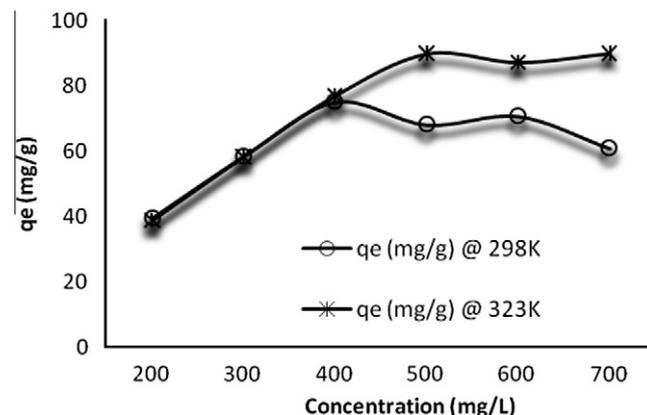
**Fig. 5.** Effect of initial adsorbate concentration on $Pb^{2+}$ adsorption.

**Table 2**
Adsorption isotherms parameters.

| Isotherm | Calculated parameter | | Experiment value | | $r^2$ | |
|---|---|---|---|---|---|---|
| | 25 °C | 50 °C | 25 °C | 50 °C | 25 °C | 50 °C |
| Langmuir | $Q_o$ = 62.50 mg/g<br>$b$ = 0.19 | 90.91 mg/g<br>0.00 | $q_e$ = 70.21 mg/g | 89.81 mg/g | 0.993 | 0.999 |
| Freundlich | $n$ = 16.13<br>$K_f$ = 49.66 | 7.58<br>47.86 | | | 0.588 | 0.719 |
| D–R. | $X_m$ = 53.46 mg/g | 55.48 mg/g | $q_t$ = 70.21 mg/g | 89.81 mg/g | 0.237 | 0.554 |

D–R. = Dubinin–Radushkevich.

## 3.5. Adsorption isotherms and thermodynamics

The effects of sorbate concentrations and temperature on adsorption were done using varying $Pb^{2+}$ concentrations between 200 and 700 mg/L at 25 ± 2 °C and 50 ± 2 °C. Results (Fig. 5) show that increase in reaction temperature from 298 to 323 K, did not seem to affect amount of $Pb^{2+}$ adsorption onto the surface of RBL at lower concentrations until maximum sorption which occurred at 400 mg/L of $Pb^{2+}$ concentration in solution. Then increase in temperature led to an increase in the amount of $Pb^{2+}$ metal adsorbed (from ≈77 mg/g to ≈90 mg/g) as concentration of the metal increased from 400 mg/L to 500 mg/L, while there was no noticeable change in amount of $Pb^{2+}$ metal adsorbed at 298 K. Thus, temperature enhanced the reactions between of $Pb^{2+}$ ions and the RBL surface functional groups. However, further increase in $Pb^{2+}$ concentration at the higher temperature did not cause any increase in adsorption. Thus, to increase rate and efficiency of adsorption of $Pb^{2+}$ on RBL as well as reduce the effect of the repulsive forces discussed in Section 3.3, high reaction temperature is recommended.

Langmuir, Freundlich and Dubinin–Radushkevich sorption isotherms (Table 2) were used to assess the RBL adsorption capacity and surface sorption properties. Langmuir isotherm, which is based on the assumption that all sites possess equal affinity for the sorbate while forming a sorbate monolayer on the biosorbent surface at saturation, gave better fit to the sorption data than the Freundlich model which assumes sorption on heterogeneous surfaces [4]. The Dubinin–Radushkevich sorption isotherm which combines both assumptions did not fit the sorption data. The estimated monolayer adsorption capacity ($Q_o$) is 62.50 and 90.91 mg/g at 298 K and 323 K respectively.

Table 3 shows the thermodynamic parameters obtained. The free energy changes ($\Delta G^o$) were positive with values of 76.8 kJ/mol and 83.3 kJ/mol at 298 K and 323 K respectively. The calculated values of enthalpy $\Delta H^o$ were positive and imply that the reaction is an exothermic process and releases energy. As the diffusion process was exothermic in nature, it is expected that increased solution temperature would result in decreased uptake of $Pb^{2+}$ ions from aqueous solution. However, energy is needed to break the repulsive forces hindering further $Pb^{2+}$ adsorption and thus higher temperature led to higher adsorption. The entropy $\Delta S^o$ of the reaction was negative due to the fact that the displaced molecules from RBL surfaces lost more translational entropy than was gained by the $Pb^{2+}$ ions, thus, there will be decreased randomness at the RBL/solution interface.

**Table 4**
Review of maximum sorption capacity ($Q_{max}$) for $Pb^{2+}$ sorption by different biosorbents reported in the literature.

| Biomass | $Pb^{2+}$ $Q_{max}$ (mg/g) | Ref. |
|---|---|---|
| Modified orange peel | 476.1 | [29] |
| Ulva sp. | 302.5 | [31] |
| Padina sp. | 259.0 | [31] |
| Sargassum sp. | 240.4 | [31] |
| Waste maize bran | 142.86 | [32] |
| Orange peel | 113.5 | [29] |
| Lignin | 102.40 | [8] |
| Gracilliiaria sp. | 93.2 | [31] |
| RBL | 89.8 at 323 K | Present study |
| Tea leaves | 78.87 | [9] |
| RBL | 70.21 at 298 K | Present study |
| Sago | 46.60 | [33] |
| Tree fern | 40.00 | [10] |
| Groundnut husks | 39.40 | [11] |
| Sphagnum moss peat | 30.70 | [12] |
| Hazelnut shell | 28.18 | [6] |
| Sawdust | 21.05 | [13] |
| Rice hulls | 11.40 | [34] |
| Chitosan | 8.31 | [14] |
| Almond shell | 8.08 | [6] |

The $Pb^{2+}$ adsorption capacities of some alternative biosorbents reported in literature have been tabulated in Table 4 and compared with that of RBL. It shows that RBL adsorption capacity is much higher than most biosorbents reported in literature. Thus, its good adsorption capacity, ease of sample treatment, as well as availability makes RBL a promising cost-effective biosorbent for $Pb^{2+}$ removal from aqueous environment.

## 4. Conclusion

The ability of *B. lambarenensis* biosorbent to remove $Pb^{2+}$ from aqueous solution was investigated in equilibrium, kinetics and thermodynamics studies. The results obtained show that the biomass of *B. lambarenensis* has an optimum pH for $Pb^{2+}$ adsorption at 5.0, nearly attains maximum adsorption within 1 h at 298 K, and obeys the pseudo-second order kinetics with an exothermic reaction. $Pb^{2+}$ adsorption increased with increase in temperature. The Langmuir isotherm described the equilibrium data better than other isotherms indicating adsorption is monolayer with monolayer adsorption capacity of 62.50 mg/g at 298 K and 90.91 mg/g at 323 K. The FT-IR analysis showed that possible functional groups responsible for metal adsorption are carboxyl, carbonyl, amides, hydroxyl and possibly other smaller groups that cannot be identified using only FT-IR spectra. Taking into account its good adsorption capacity, ease of sample treatment, as well as availability, the biomass of *B. lambarenensis* is a promising cost-effective biosorbent for $Pb^{2+}$ removal from aqueous environment.

**Table 3**
Thermodynamic parameters for $Pb^{2+}$ adsorption process.

| | $T$ = 298 K | $T$ = 323 K |
|---|---|---|
| $\Delta G^o$ (KJ/mol) | 76.8 | 83.3 |
| $\Delta H^o$ (KJ/mol) | −30315.6 | −32858.8 |
| $\Delta S^o$ (KJ/mol) | −0.258 | −0.258 |

## References

[1] E.I. Unuabonah, B.I. Olu-Owolabi, K.O. Adebowale, A.E. Ofomaja, Adsorption of lead and cadmium ions from aqueous solutions by tripolyphosphate–impregnated Kaolinite clay, Colloids Surf. A: Physicochem. Eng. Asp. 292 (2007) 202–211.

[2] M.N.M. Ibrahim, W.S.W. Ngah, M.S. Norliyana, W.R.W. Daud, M. Rafatullah, O. Sulaiman, et al., A novel agricultural waste adsorbent for the removal of lead (II) ions from aqueous solutions, J. Hazard. Mater. 182 (2010) 377–385.

[3] T.A. Kurniawan, G.Y.S. Chan, W. Lo, S. Babel, Comparisons of low-cost adsorbents for treating wastewaters laden with heavy metals, Sci. Total Environ. 366 (2006) 409–426.

[4] C. Yan, G. Li, P. Xue, Q. Wei, Q. Li, Competitive effect of Cu(II) and Zn(II) on the biosorption of lead(II) by *Myriophyllum spicatum*, J. Hazard. Mater. 179 (2010) 721–728.

[5] A. Saeed, M. Iqbal, W.H. Holl, Kinetics, equilibrium and mechanism of $Cd^{2+}$ removal from aqueous solution by mungbean husk, J. Hazard. Mater. 168 (2009) 1467–1475.

[6] E. Pehlivan, T. Altun, S. Cetin, M.I. Bhanger, Lead sorption by waste biomass of hazelnut and almond shell, J. Hazard. Mater. 167 (2009) 1203–1208.

[7] A.E. Ofomaja, E.B. Naidoo, S.J. Modise, Removal of copper(II) from aqueous solution by pine and base modified pine cone powder as biosorbent, J. Hazard. Mater. 168 (2009) 909–917.

[8] X. Guo, S. Zhang, X. Shan, Adsorption of metal ions on lignin, J. Hazard. Mater. 151 (2008) 134–142.

[9] W.T. Tan, M.K. Abd Rahman, Removal of lead, cadmium and zinc by waste tea leaves, Environ. Technol. Lett. 9 (1998) 1223–1232.

[10] Y.S. Ho, W.T. Chiu, C.S. Hsu, C.T. Huang, Sorption of lead ions from aqueous solution using tree fern as a sorbent, Hydrometallurgy 73 (2004) 55–61.

[11] F.E. Okieimen, E.U. Okundia, D.E. Ogbeifun, Sorption of cadmium and lead ions on modified groundnut (*Arachis hypogea*) husks, J. Chem. Technol. Biotechnol. 51 (1991) 97–103.

[12] Y.S. Ho, D.A.J. Wase, C.F. Forster, Kinetic studies of competitive heavy metal adsorption by sphagnum moss peat, Environ. Technol. 17 (1996) 71–77.

[13] Q. Li, J. Zhai, W. Zhang, M. Wang, J. Zhou, Kinetic studies of adsorption of Pb(II), Cr(III) and Cu(II) from aqueous solution by sawdust and modified peanut husk, J. Hazard. Mater. 141 (2007) 163–167.

[14] M.M.D. Zulkali, A.L. Ahmad, N.H. Norulakmal, N.S. Sharifah, Comparative studies of *Oryza sativa* L. husk and chitosan as lead adsorbent, J. Chem. Technol. Biotechnol. 81 (2006).

[15] K.A. Krishnan, T.S. Anirudhan, Removal of cadmium(II) from aqueous solutions by steam-activated sulphurised carbon prepared from sugar-cane bagasse pith: kinetics and equilibrium studies, Water SA 29 (2003) 147–156.

[16] N. Meunier, J. Laroulandie, J.F. Blais, R.D. Tyagi, Cocoa shells for heavy metal removal from acidic solutions, Biores. Technol. 90 (2003) 255–263.

[17] M. Ajmal, R.A.K. Rao, S. Anwar, J. Ahmad, R. Ahmad, Adsorption studies on rice husk: removal and recovery of Cd(II) from wastewater, Biores. Technol. 86 (2003) 147–149.

[18] A.O. Ogunfowokan, O.I. Asubiojo, A.A. Adeniyi, E.A. Oluyemi, Trace Pb, Zn, and Cu in *Barbula Lambarenensis* as a monitor of local atmospheric pollution in Ile-Ife, Nigeria, J. Appl. Sci. 4 (2004) 380–383.

[19] G.W. Sears, Determination of specific surface area of colloidal silica by titration with sodium hydroxide, Anal. Chem. 28 (1956) 1981–1983.

[20] R.K. Iler, The Chemistry of Silica, John Wiley & Sons, New York, 1979. pp. 203–206, 243.

[21] M. Radojevic, V.N. Bashkin, Practical Environmental Analysis, Royal Society of Chemistry, Cambridge, 1998.

[22] E.I. Unuabonah, K.O. Adebowale, B.I. Olu-Owolabi, L.Z. Yang, L.X. Kong, Adsorption of Pb (II) and Cd (II) from aqueous solution onto sodium tetraborate–modified Kaolinite clay: equilibrium and thermodynamic studies, Hydrometallurgy 93 (2008) 1–9.

[23] G. Sposito, The Chemistry of Soils, Oxford University Press, New York, NY, 1989.

[24] M. Mohammad, S. Maitra, N. Ahmad, A. Bustam, T.K. Sen, B.K. Dutta, Metal ion removal from aqueous solution using physic seed hull, J. Hazard. Mater. 179 (2010) 363–372.

[25] S. Lagergren, About the theory of so-called adsorption of soluble substances, Kungliga Svenska Vetenskapsakademiens Handlingar 24 (1898) 1–39.

[26] E. Demirbas, M. Kobya, E. Senturk, T. Ozkan, Adsorption kinetics for the removal of chromium (VI) from aqueous solutions on the activated carbons prepared from agricultural wastes, Water SA 30 (2004) 533–5400.

[27] S. Chakravarty, A. Mohanty, T.N. Sudha, A.K. Upadhyay, J. Konar, J.K. Sircar, et al., Removal of Pb(II) ions from aqueous solution by adsorption using bael leaves (*Aegle marmelos*), J. Hazard. Mater. 173 (2010) 502–509.

[28] Z.-Y. Yao, J.-H. Qi, L.-H. Wang, Equilibrium, kinetic and thermodynamic studies on the biosorption of Cu(II) onto chestnut shell, J. Hazard. Mater. 174 (2010) 137–143.

[29] N. Feng, X. Guo, S. Liang, Y. Zhu, J. Liu, Biosorption of heavy metals from aqueous solutions by chemically modified orange peel, J. Hazard. Mater. 185 (2011) 49–54.

[30] M.A. Tofighy, T. Mohammadi, Adsorption of divalent heavy metal ions from water using carbon nanotube sheets, J. Hazard. Mater. 185 (2011) 140–147.

[31] P.X. Sheng, Y. Ting, J.P. Chen, L. Hong, Sorption of lead, copper, cadmium, zinc, and nickel by marine algal biomass: characterization of biosorptive capacity and investigation of mechanisms, J. Colloid Interface Sci. 275 (2004) 131–141.

[32] K.K. Singh, A.K. Singh, S.H. Hasan, Low cost biosorbent 'wheat bran' for the removal of cadmium from wastewater: kinetic and equilibrium studies, Bioresour. Technol. 97 (2006) 994–1001.

[33] S.Y. Quek, D.A.J. Wase, C.F. Forster, The use of sago waste for the sorption of lead and copper, Water SA 24 (1998) 251–256.

[34] M.N.V. Prasad, H. Freitas, Removal of toxic metals from solution by leaf, stem and root phytomass of *Quercus ilex* L. (holly oak), Environ. Pollut. 110 (2000) 277–283.